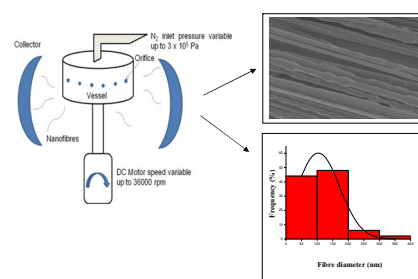# Forming of Polymer Nanofibers by a Pressurised Gyration Process

Suntharavathanan Mahalingam, Mohan Edirisinghe*

A new route consisting of simultaneous centrifugal spinning and solution blowing to form polymer nanofibers is reported. The fiber diameter (60–1000 nm) is shown to be a function of polymer concentration, rotational speed, and working pressure of the processing system. The fiber length is dependent on the rotational speed. The process can deliver 6 kg of fiber per hour and therefore offers mass production capabilities compared with other established polymer nanofiber generation methods such as electrospinning, centrifugal spinning, and blowing.

1. Introduction

Polymer nanofibers are a promising class of materials for various applications, including electronics, optical devices, batteries, and filtration.[1–9] Indeed, due to their high surface area to volume ratio, they are attractive in many biomedical applications such as scaffolds used in tissue engineering, drug release, artificial organs, wound healing and vascular grafts.[10,11] Due to the expanding demand for nanofibers across a wide range of industries, there needs to be an improvement in the current state-of-art technologies to mass produce them more consistently, reliably, robustly and cost effectively.[12]

Electrospinning is a well-established technique to generate a wide variety of polymeric fibers across the micro- to nanometer-scale range.[13,14] However, this method requires high voltage (kV range) and shows poor cost-yield efficiency as a single fiber emerges from the end of the nozzle carrying a polymeric solution. Centrifugal spinning has the ability to produce homogeneous nanofibers from poorly electrospinnable materials. It only uses the centrifugal

force in a rotary mould as rotation shears the polymer solution to form fibers.[15,16] Indeed, it is independent of solution properties such as electrical conductivity and dielectric constant which govern electrospinning, but the process is limited by complicated spinneret design which can lead to large differences in fiber quality and productivity. On the other hand, solution/melt blowing is a proven large-scale method to form a web of polymeric fibers. It involves extruding polymer solution/melt through a narrow orifice under high air velocity. The drag of high-velocity air on the surface of the polymer melt causes the polymer to elongate into fibers. The size of the fibers obtained in this process lies in the micrometer range.[17,18]
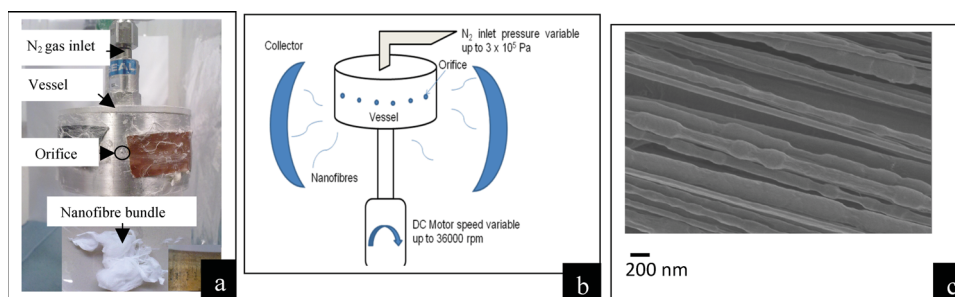
The present work uncovers a new route to process well characterised and well aligned polymeric nanofibers using the combination of centrifugal spinning and solution blowing. This technique offers not only the manipulation of the fiber diameter but also fiber diameter distribution and fiber length.

2. Experimental Section

The experimental set up operating at ambient temperature (≈20 °C) used in this study is shown in Figure 1. It consists of a rotary aluminium cylindrical vessel (≈60 mm in diameter and ≈35 mm in height) containing orifices (≈20) on its face. The size of one orifice is 0.5 mm. The vessel and orifice dimensions (including the number of orifices) can be varied to suite. One end of the vessel is connected to a motor which can generate speeds up to 36 000 rpm. The

S. Mahalingam, Prof. M. Edirisinghe
Department of Mechanical Engineering, University College London (UCL), London WC1E 7JE, UK
E-mail: m.edirisinghe@ucl.ac.uk

Figure 1. a) Actual experimental set up of the pressurised gyration process to form polymeric nanofibers and an example of a nanofiber bundle produced. The vessel containing polymer solution rotates about the vertical axis, concurrently N_2 is blown in to the vessel. The variation in the speed of the vessel and the N_2 pressure changes the diameter, length and diameter distribution of the fabricated nanofibers. b) Schematic depiction of the experimental set-up. c) Scanning electron micrograph of the nanofibers produced at a rotating speed of 36 000 rpm and a working pressure of 3×10^5 Pa.

other end is connected to a gas stream (in this work N_2), the pressure of which can be varied up to 3×10^5 Pa. The high speed of the rotating vessel forms a polymer jet. This jet subsequently stretches into fibers through an orifice. This stretching can be enhanced by blowing of gas into the vessel. To facilitate the collection of polymeric fibers, there is a stationary collector made out aluminium foil placed around the spinning vessel. It is also possible to change the collector material and this can be helpful in further increasing the yield and to deposit more complex fiber architectures.

For this investigation, polyethylene oxide (PEO; $\overline{M}_w$ 200 000 g mol^{-1}; Sigma Aldrich, Poole, UK) was used as the polymer. Three different weight percentages (5, 15, and 21 wt%) of polymer were dissolved in deionised water. The solutions were magnetically stirred at the ambient temperature for 24 h before processing. The concentrations of PEO chosen in this work were based on the viscoelastic nature of the polymer. Generally, a lower concentration promotes bead or droplet formation and a higher concentration results in polymer melt where extrusion of fibers is difficult or promotes thicker fiber formation.[19]

Surface tension and the viscosity of the polymer solution were measured using a KRUSS Tensiometer and a Brookfield viscometer, respectively. The measured values of surface tension were 50, 52, and 57 mNm^{-1} and the measured values of viscosity were 75, 2200 and 3000 mPa s for 5, 15, and 21 wt% of PEO solutions, respectively. The process was observed using a high-speed camera (Phantom v7.3, Vision Research).

Videos showing the initiation of the instability and the subsequent generation of the fibers in the process can be found online.[20]

The fibers formed were studied using field emission scanning electron microscopy (model JSM 6301 F). Before imaging, the samples were coated with gold using a sputtering machine (Edwards Sputter S1 50B) for 90 s to minimize charging effects. The fiber diameter was obtained using high-magnification images with IMAGE J software using ≈100 measurements.

3. Results and Discussion

The formation of nanofibers in this technique could be explained by invoking the Rayleigh–Taylor instability on the liquid jet emerging from polymer solution. The external driving force is the gravitational force when a polymer drop emerges from the orifice. There will be a surface tension gradient along the liquid–air interface separating the drop from the surrounding air. The Marangoni stress due to the surface tension gradient, which is tangential to the liquid/gas interface induces a flow from the top to the tip of the polymer drop.[21] The instability between the liquid/gas interface could be determined by equating the destabilising gravitational force per unit volume to the stabilising surface tension force per unit volume.[22]

$$\rho g \frac{\partial h}{\partial x} = \gamma \frac{\partial^3 h}{\partial x^3} \tag{1}$$
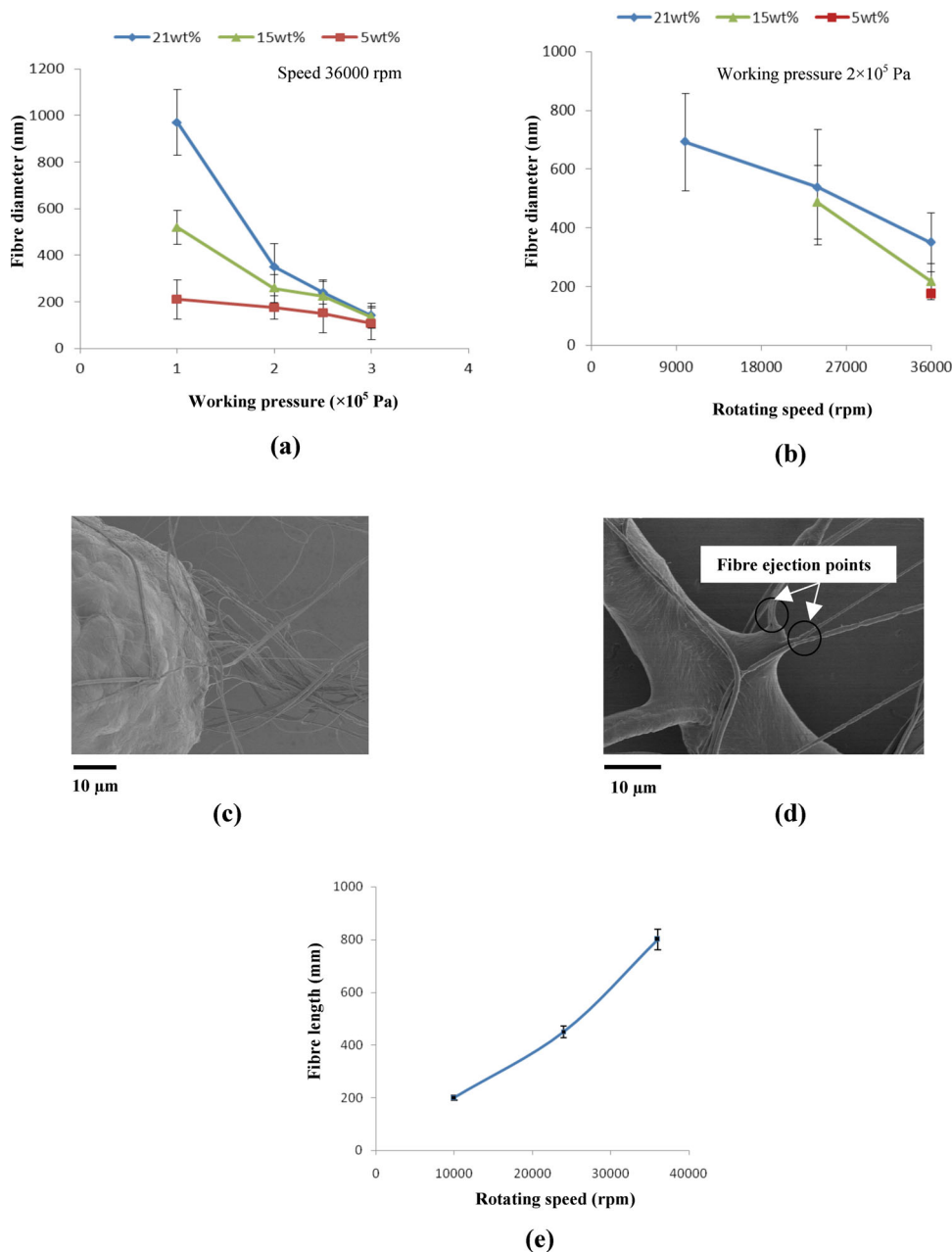
Here, g is the gravitational force, ρ is density of the polymer solution, γ is the liquid–gas surface tension, h is the height of the liquid drop hanging under the horizontal surface and x is the vertical distance.

During spinning and gas blowing action, Equation 1 is replaced by the destabilising centrifugal force ($\rho \omega^2 R$) and pressure difference at orifice (Δp) instead of the gravitational force. ω is rotational speed and R is the radius of the vessel. From this, the characteristics length scale of the instability is:

$$L = \left[\frac{h\gamma}{(\rho \omega^2 R) + \Delta p} \right]^{1/3} \tag{2}$$

Fiber formation from this process could be explained by the following steps. Initially, a jet emerges from the orifice on the face of the vessel. This jet further stretches due to the centrifugal force and the pressure difference at the orifice. Finally, the evaporation of the solvent leads to thinning of the fibers formed. The reason for only jet formation instead of droplets in this classical surface instability is viscoelasticity of the polymer solution used.
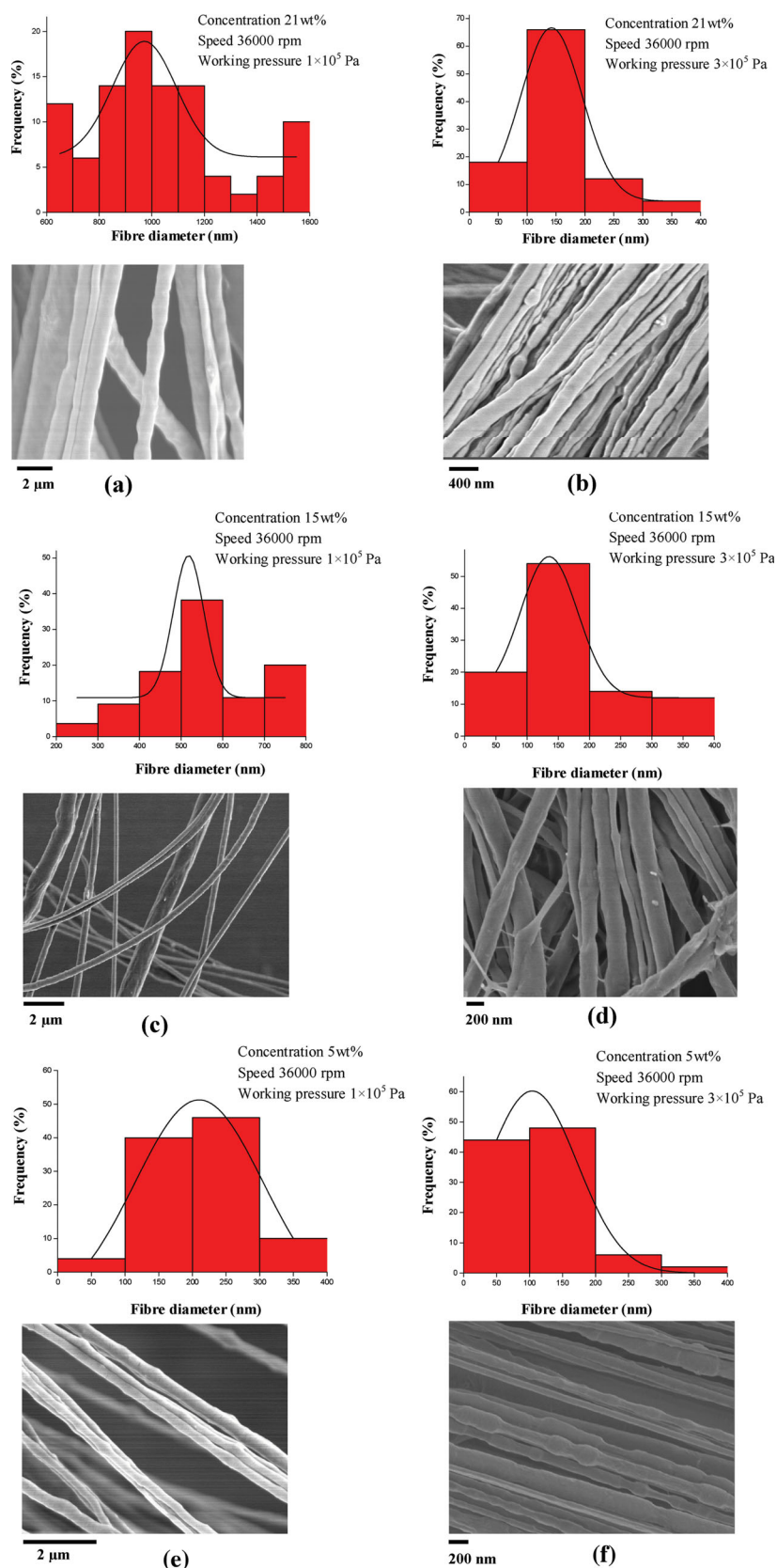
The rotating speed, working pressure and polymer concentration were varied to study the effect on the fiber diameter. Figure 2a shows the plot of fiber diameter

(a)

(b)

(c)

(d)

(e)

Figure 2. a) Fiber diameter variation with working pressure for 21, 15, and 5 wt% of PEO solutions at a fixed rotational speed of 36 000 rpm. b) Fiber diameter variation with rotational speed for 21, 15, and 5 wt% of PEO solution at a fixed working pressure of 2× 10⁵ Pa. c) The emergence of polymer fibers from a PEO bead due to Rayleigh–Taylor instability at a rotational speed of 24 000 rpm. d) Shearing and thinning of polymer fibers due to increase of rotational speed to 36 000 rpm. e) Fiber length variation with rotational speed.

against the working pressure of the processing system. Fibers in the range of 1000 to 60 nm were produced. A dramatic reduction in fiber diameter was observed by increasing the working pressure from 1×10^5 to 3×10^5 Pa. Thus, for the 21 wt% of PEO solution, increasing the working pressure from 1×10^5 to 3×10^5 Pa, the fiber diameter reduced from 970 to 141 nm at a rotating speed of 36 000 rpm. Similarly, for the 15 wt% of PEO solution,

the fiber diameter reduced from 518 to 135 nm, and for the 5 wt% of PEO solution, from 210 to 106 nm. At a lower working pressure, the fiber diameter difference is high between the different polymer concentrations. However, the difference is very narrow at the higher working pressure. This is due to differences in viscosity of the polymeric solutions and the rate of evaporation of solvent during processing.[14] Increasing the rotational

www.MaterialsViews.com

Figure 3. a–f) Fiber diameter distributions and corresponding electron micrograph images of the products for 21, 15, and 5 wt% of PEO solutions.

speed to 24 000 rpm gives no fiber formation in the 5 wt% of PEO solution, only polymer beads were found. However, at the speed of 36 000 rpm, the measured fiber diameter was 175 nm. For the 15 wt% PEO solution, the fibers were formed at a rotational speed of 24 000 rpm and the fiber diameter was reduced with rotational speed. The same is true for the 21 wt% of PEO solution where fiber diameter was reduced from 692 to 350 nm as the rotational speed increased from 10 000 to 36 000 rpm (Figure 2b). Figure 2c shows the evolution of fibers from a polymer bead for 15 wt% of PEO solution at a rotational speed of 24 000 rpm. The polymer bead is connected to numerous fibers. Figure 2d shows the shearing and thinning of the fibers at a rotational speed of 36 000 rpm for the same PEO solution. This observation shows that there should be a minimum rotational speed to form fibers at a low polymer concentration. By taking $h = 40 \mu m$, $\gamma = 52 \, mNm^{-1}$, $\omega = 3771 \, s^{-1}$, $R = 30 \, mm$, $\rho = 1000 \, kg \, m^{-3}$ and $\Delta p = 2 \times 10^5$ Pa, the wavelength of instability can be calculated using Equation 2 and $L = 17 \mu m$. It is also clearly seen that the mean distance between the points of ejection of polymer fibers from the droplet is in a good agreement with the theoretically predicted value L (Figure 2d). Moreover, fiber stretching (length of the fibers) is also influenced by rotational speed of the spinneret. A fiber length of ≈ 200 mm is obtained for a rotational speed of 10 000 rpm where a fiber length of ≈ 800 mm is obtained for a rotational speed of 36 000 rpm (Figure 2e).

Figure 3a–f shows the fiber diameter distribution for different processing conditions. It is evident that at 21 wt% of polymer and a lower working pressure, a wider size distribution of fibers is obtained. The mean fiber diameter is reduced when increasing the working pressure. A similar observation is found for 15 wt% of polymer solution. The polydispersity index (standard deviation/mean) of the distribution for these two cases is 13% and 14%, respectively, at a lower working pressure of 1×10^5 Pa. At a higher working pressure of 3×10^5 Pa the

polydispersity index is 38% and 34% for 21 and 15 wt% polymer solutions, respectively. For 5 wt% of PEO solution, a polydispersity index of 40% and 63% is found for 1×10^5 and 3×10^5 Pa working pressure, respectively. This observation shows that the formed fiber diameter and distribution could be controlled through this forming technique. In all cases, well-aligned and bead-free fibers were produced at a higher rotational speed. However, at a lower rotational speed, some beaded fibers were formed due to lack of shear force. This suggests that this technique can offer formation of tailor made nanofibers for various applications. A distinct advantage of this technique compared with electrospinning is a significant reduction in the random orientation of fibers formed. This is largely due to the non-existence of whipping or non-axisymmetric instabilities.[23] In the absence of an electric field, the non-existence of repulsive forces brought about by surface charges can help to form well-ordered nanofibers.

The competition between the centrifugal force and pressure difference at the orifice against the surface tension of the polymeric solution is responsible for fiber formation in this process. The centrifugal force accelerates the liquid stream where solvent evaporation and polymer chain elongation occurs.[16] This acceleration is enhanced by the gas blowing operation where liquid exerts more force to overcome the surface tension force. By considering the Matsui model,[24] the relationship between air drag coefficient (C_f) and fiber diameter can be obtained. $C_f = 0.37 \times N_{Re}^{-0.61}$, where N_{Re} is the Reynolds number ($= \frac{DV\rho}{\eta}$), D is the fiber diameter, V is the gas velocity, ρ is the nitrogen density and η is the dynamic viscosity of nitrogen. Taking $C_f = 1$, $\rho = 1.25$ kg m^{-3}, $\eta = 18.6$ µPa s and $V = 30$ ms^{-1}, the fiber diameter is predicted to be ≈100 nm. As the jet leaves the orifice, the elongational flow dominates and significantly affects the molecular stretching. The change in velocity along the streamlines and the difference of velocity at the ends of the molecular chain reduces the cross-sectional area of the jet to be drawn.[24] Thus, this combined force induces greater extension and thinning of the polymeric jet forming finer fibers at higher working pressure and rotational speed. Further, blowing of air will facilitate the evaporation of the solvent by diffusion of solvent through polymer to the surface, thus assisting the production of finer fibers.

As shown earlier, by varying the processing conditions, the fiber diameter could be controlled in this technique for various PEO concentrations. It is further illustrated that there needs to be a critical condition to prepare fibers from this technique, otherwise polymer beads will be produced. It is well known that polymer molecular weight and polymer chain entanglement significantly affect the fiber morphologies.[25] Fabricating continuous fiber morphologies require a minimum molecular weight to allow sufficient polymer entanglement, or for a given

molecular weight, the entanglement density increases with concentration of the polymer and minimises 'bead on string' fiber morphology.[26] The minimum molecular weight determines the critical chain overlap concentration. Fiber morphologies are shown to be greatly affected by critical chain overlap concentration.[27] Thus, as the polymer concentration increases, the overlapping of polymer chains form sufficient entanglement networks of polymer chains. Bead-free continuous fibers are formed when the polymer concentration is above the critical concentration. However, increasing the concentration of the polymer increases the viscosity of polymer solution hindering solvent evaporation, and this results in thicker fibers or solidification takes place during spinning and the fibers cannot be formed. If the concentration of polymer is too low, only droplets or beads will be formed or bead on string fibers will be promoted.

The viscoelasticity of the polymer solution is a well-known property of any polymeric system. It is a time dependent property expressing the viscosity of liquid and the elasticity of a polymer system. This property is influenced by the external force and time constant during which that force is exerted on the polymer solution. For non-Newtonian flow, the shear stress τ is proportional to the rate of shear $\dot{\gamma}^n$ where n is a constant.[28] The increase of the rotational speed during spinning will increase the centrifugal force. This in turn reduces the time constant of forces acting on the polymer solution. Smaller the time constant, the more elastic is the response of the polymer chains. Conversely, higher the time constant, the viscous response of the polymer increases, and therefore there is a need to have a minimum rotational speed to increase the viscous response of the polymer solution for fabrication of the fibers from the low concentration of polymer solution. This is the reason behind bead formation for 5 and 15 wt% of PEO solution at low rotational speed. Moreover, in non-Newtonian liquids, the existence of normal stresses in contrast to shear stresses represents stresses in the same direction as the deformation plane. This facilitates more stretching of the polymer drawn from the orifice.[24] Although the pressurised gyration process takes place at the ambient temperature, the temperature of the polymeric jet changes as the solvent evaporates. There is a temperature gradient arising through the polymeric jet at given time. Even at ambient temperature, a higher rotational speed facilitates solvent evaporation through frictional and heat loss which inevitably affects the elongational viscosity. The change in elongational viscosity during spinning determines the final fiber diameter and the distribution.

The fiber diameter and yield of this technique is compared with each individual technique and electrospinning (Table 1). It is clearly seen that this new

▌ Table 1. Comparison of fiber diameter and yield for different techniques.

Technique	Yield [kg h⁻¹]	Fiber diameter [nm]
Centrifugal spinning[12,27]	0.06	45–400
Solution blowing[17,29]	7–8	1000
Electrospinning[12]	0.17	50
Present work (pressurised gyration)[a]	6	60–1000

[a]Calculated on the basis of preparing fibers from 1 g of solution

technique provides a higher yield than the centrifugal spinning technique and the electrospinning method. The yield is very much comparable to the solution blowing method. On the other hand, the nanofibers produced could be as small as 60 nm and very much comparable to the commercialised centrifugal and electrospinning techniques. Also, this method will pave the way to fine-tune the nanofiber diameter and the diameter distribution in a more efficient way.

4. Conclusions

A hybrid technique consisting of simultaneous centrifugal spinning and solution blowing has been innovated to generate fibers in the range of 60–1000 nm. It is electro- and/or magnetic-field-free and a nozzle-free technique applicable to fabricate nanofibers in the large scale. It is a simple and effective technique independent of electrical conductivity and dielectric constant of the materials from which nanofibers are generated. In addition, this method offers the production of well-characterised bead-free fibers in a well-aligned direction by varying the working pressure, rotating speed and concentration of the polymeric solution.

[1] S. Chaudhari, M. Srinivasan, *J. Mater. Chem.* **2012**, *22*, 23049.
[2] M. Li, J. Zhang, H. Zhang, Y. Liu, C. Wang, X. Xu, Y. Tang, B. Yang, *Adv. Funct. Mater.* **2007**, *17*, 3650.
[3] A. A. Sagade, K. Venkata Rao, U. Mogera, S. J. George, A. Datta, G. U. Kulkarni, *Adv. Mater.* **2012**, *25*, 559.
[4] V. Vohra, U. Giovanelle, R. Tubino, H. Murata, C. Botta, *ACS Nano* **2011**, *5*, 5572.
[5] Y. Li, B. K. Guo, L. W. Ji, Z. Lin, G. J. Xu, Y. Liang, S. Zhang, O. Toprakci, Y. Hu, M. Alcoutlabi, X. W. Zhang, *Carbon* **2013**, *51*, 185.
[6] Y. Li, C. W. Joo, *J. Appl. Polym. Sci.* **2012**, *126*, E252.
[7] S. Sinha-Ray, Y. Zhang, A. L. Yarin, *Langmuir* **2011**, *27*, 215.
[8] D. Y. Tu, S. Pagliara, R. Cingolani, D. Pisignano, *Appl. Phy. Lett.* **2011**, *98*, 023307.
[9] Y. C. Chiu, Y. Chen, C. C. Kuo, S. H. Tung, T. Kakuchi, W. C. Chen, *Appl. Mater. Interface* **2012**, *4*, 3387.
[10] Z. Huang, H. Lee, E. Lee, S. K. Kang, J. M. Nam, M. Lee, *Nat. Commun.* **2011**, *2*, 459.
[11] N. Bhardwaj, S. C. Kundu, *Biotechnol. Adv.* **2010**, *28*, 325.
[12] C. J. Luo, S. D. Stoyanov, E. Stride, E. Pelan, M. J. Edirisinghe, *Chem. Soc. Rev.* **2012**, *41*, 4708.
[13] H. B. Zhang, M. J. Edirisinghe, *J. Am. Ceram. Soc.* **2006**, *89*, 1870.
[14] D. Petras, P. Slobodian, V. Pavlinek, P. Saha, D. Kimmer, *AIP Conf. Proc.* **2011**, *1375*, 312.
[15] L. Wang, J. Shi, L. Liu, E. Secret, Y. Chen, *Microelectron Eng.* **2011**, *88*, 1718.
[16] M. R. Badrossamay, H. A. McIlwee, J. A. Goss, K. K. Parker, *Nano Lett.* **2010**, *10*, 2257.
[17] E. S. Medeiros, G. M. Glenn, A. P. Klamczynski, W. J. Orts, *J. Appl. Polym. Sci.* **2009**, *113*, 2322.
[18] R. G. Zhao, L. C. Wadsworth, *Polym. Eng. Sci.* **2003**, *43*, 463.
[19] D. S. Katti, K. W. Robinson, F. K. Ko, C. T. Laurencin, *J. Biomed. Mater. Res., Part B* **2004**, *70*, 286.
[20] a) http://www.youtube.com/watch?v=9uUXk587u_0 (accessed May, 2013); b) http://www.youtube.com/watch?v=51vAdaZZzWI (accessed May, 2013).
[21] R. Suryo, O. A. Basaran, *Phy. Rev. Lett.* **2006**, *96*, 034504.
[22] R. T. Weitz, L. Harnau, S. Rauschenbach, M. Burghard, K. Kern, *Nano Lett.* **2008**, *8*, 1187.
[23] J. A. Ajao, A. A. Abionao, S. Chigome, A. Y. Fasasi, G. A. Osinkolu, M. Maaza, *J. Mater. Sci.* **2010**, *45*, 2324.
[24] V. B. Gupta, V. K. Kothari, *Manufactured Fiber Technology*, Chapman & Hall, London **1997**, pp 201.
[25] C. J. Luo, E. Stride, S. D. Stoyanov, E. Pelan, M. J. Edirisinghe, *J. Polym. Res.* **2011**, *18*, 2515.
[26] S. L. Shenoy, W. D. Bates, H. L. Frisch, E. Pelan, G. E. Wnek, *Polymer* **2005**, *46*, 3372.
[27] P. Gupta, C. Elkins, T. E. Long, G. L. Wilkes, *Polymer* **2005**, *46*, 4799.
[28] A. Ram, *Fundamental of Polymer Engineering*, Plenum Press, London **1997**, pp 58.
[29] S. Malkan, *Tappi J.* **1995**, *78*, 185.

Makerials Views
www.MaterialsViews.com

Macromol. Rapid Commun. **2013**, *34*, 1134–1139
© 2013 The Authors. Published by WILEY-VCH Verlag GmbH & Co. KGaA, Weinheim

Macromolecular Journals

1139